Published in final edited form as:
Exp Brain Res. 2008 July ; 189(1): 35–47. doi:10.1007/s00221-008-1401-1.

Coordination of eye and head components of movements evoked by stimulation of the paramedian pontine reticular formation

Neeraj J. Gandhi,
Department of Neuroscience, Baylor College of Medicine, Houston, TX 77030, USA

Departments of Otolaryngology, Bioengineering, and Neuroscience, Center for the Neural Basis of Cognition, University of Pittsburgh, Pittsburgh, PA 15213, USA

Department of Otolaryngology, Eye and Ear Institute, Room 108, University of Pittsburgh, 203 Lothrop Street, Pittsburgh, PA 15213, USA

Ellen J. Barton, and
Department of Neuroscience, Baylor College of Medicine, Houston, TX 77030, USA

David L. Sparks
Department of Neuroscience, Baylor College of Medicine, Houston, TX 77030, USA

Neeraj J. Gandhi: neg8@pitt.edu

Abstract

Constant frequency microstimulation of the paramedian pontine reticular formation (PPRF) in head-restrained monkeys evokes a constant velocity eye movement. Since the PPRF receives significant projections from structures that control coordinated eye-head movements, we asked whether stimulation of the pontine reticular formation in the head-unrestrained animal generates a combined eye-head movement or only an eye movement. Microstimulation of most sites yielded a constant-velocity gaze shift executed as a coordinated eye-head movement, although eye-only movements were evoked from some sites. The eye and head contributions to the stimulation-evoked movements varied across stimulation sites and were drastically different from the lawful relationship observed for visually-guided gaze shifts. These results indicate that the microstimulation activated elements that issued movement commands to the extraocular and, for most sites, neck motoneurons. In addition, the stimulation-evoked changes in gaze were similar in the head-restrained and head-unrestrained conditions despite the assortment of eye and head contributions, suggesting that the vestibuloocular reflex (VOR) gain must be near unity during the coordinated eye-head movements evoked by stimulation of the PPRF. These findings contrast the attenuation of VOR gain associated with visually-guided gaze shifts and suggest that the vestibulo-ocular pathway processes volitional and PPRF stimulation-evoked gaze shifts differently.

Keywords

Gaze shifts; PPRF; Saccade; Superior colliculus; Head movements; Spinal cord

Correspondence to: Neeraj J. Gandhi, neg8@pitt.edu.

Introduction

The generation of head-restrained saccades requires a spatial to temporal transformation of the neural activity along the oculomotor neuraxis (see Sparks and Gandhi 2003 for a review). Neurons in the cortical eye fields and the superior colliculus are topographically organized, such that the locus of the active population encodes the desired change in gaze. The place code signal is transformed into a temporal code downstream at the level of the paramedian pontine reticular formation (PPRF), which produces the horizontal component of saccades, and the midbrain/diencephalon junction, which controls the vertical and torsional components. Most burst neurons in the PPRF, notably the putative excitatory burst neurons that project to the abducens motoneurons, discharge a high-frequency burst for all saccades with an ipsiversive horizontal component. The number of spikes in the burst dictates the saccade amplitude (Keller 1974) and the discharge dynamics determine the velocity profile (Van Gisbergen et al. 1981).

Microstimulation is also useful for distinguishing between spatial and temporal encoding schemes. Current injected into the superior colliculus of head-restrained animals, for example, evokes a site-specific vector, provided that the stimulation duration is sufficiently prolonged (Robinson 1972; Schiller and Stryker 1972; Guitton et al. 1980). Manipulation of stimulation intensity and current changes the speed of the eye movement, but its velocity profile continues to resemble a saccade (Stanford et al. 1996). Constant frequency microstimulation of the PPRF, in contrast, moves the eyes ipsilaterally at a constant velocity for the duration of the stimulation (barring constraints placed by oculomotor range limits), and the speed of the ramp-like movement scales with stimulation frequency (Cohen and Komatsuzaki 1972).

When the head is unrestrained, the site-specific output of frontal and supplementary eye fields, as well as the superior colliculus, still encodes a desired change in gaze, but the gaze shift can now be produced as a coordinated movement of the eyes and the head (Roucoux et al. 1980; Munoz et al. 1991; Paré et al. 1994; Freedman et al. 1996; Freedman and Sparks 1997a; Tu and Keating 2000; Klier et al. 2001; Martinez-Trujillo et al. 2003; Chen and Walton 2005; Knight and Fuchs 2007). Since the extraocular and neck muscles provide independent means of producing movements, the desired gaze displacement signal must be processed separately for the extraocular and neck motoneurons. The downstream PPRF region is a potential site where the separate eye and head control pathways exist (Gandhi and Sparks 2007). Thus, the primary objectives of this study were to characterize the eye and/or head movements evoked by stimulation of the monkey PPRF; to compare the coordination of eye and head movements, should they be observed, with those recorded during visually-guided gaze shifts; and to compare the movements evoked using matched stimulation parameters in head-restrained and head-unrestrained conditions. A secondary goal, which also served as a control, was to perform the microstimulation experiments on extraocular motoneuron pools in order to confirm that movements were limited to the eyes only, even when the head was unrestrained.

Preliminary versions of this study have been published previously (Gandhi and Sparks 2000; Sparks et al. 2001).

Methods

Data were obtained from two juvenile rhesus monkeys (*Macaca mulatta*). All experimental protocols were approved by the Institutional Animal Care and Use Committee at the Baylor College of Medicine and complied with the guidelines of the Public Health Service policy on Humane Care and Use of Laboratory Animals. Surgical and behavioral procedures, as

well as the apparatus used for these experiments, have been described previously (Gandhi and Sparks 2001). Briefly, using the magnetic induction technique, gaze (eye-in-space) and head (head-in-space) positions were sampled from search coils attached to the eye and head, respectively. For each experimental session, the monkey sat in a primate chair and faced a tangent screen consisting of an array of tri-state (red, green and yellow) light emitting diodes (LEDs) in a dimly lit room. A miniature laser module, mounted on the monkey's head, projected a red beam onto the visual display. At the start of each trial, the laser was illuminated simultaneously with a red LED, located between −20° and 20° along the horizontal axis. The monkeys were granted 4,000 ms to direct the laser beam within 4–6° of the red LED and maintain the alignment for 700–1,000 ms. Next, a green LED was illuminated on the horizontal axis within 30° of the red target. The monkeys were trained to direct their gaze within 2–4° of the green target in the next 500 ms, without significantly changing their head position, and fixate for 700–1,000 ms. Next, the laser and both targets were extinguished. A yellow target was presented following a *gap period* of 100–600 ms, and the monkeys were allowed 800 ms and any combination of eye-head movement to bring gaze position within 6–10° of the stimulus. Fixation of the yellow LED for 800–1,600 ms triggered a solenoid to administer a liquid reward. When the head was restrained, the trial initiated with illumination of the green stimulus and followed the remaining steps as described above.

For each electrophysiology session, a microelectrode was lowered through a 15-mm diameter chamber slanted laterally at an angle of 26° in the frontal plane, an approach that permits access to the PPRF region, including the abducens nucleus (Gandhi and Sparks 2007). For an initial series of tracks, the penetrations were performed in the head-restrained animal; for later tracks, once the PPRF region was identified, the microelectrode was usually lowered while the head was unrestrained. The abducens nuclei were identified by their burst-tonic activity associated with saccades (Schiller 1970) and by the effects of stimulation (Reinhart and Zuber 1970). The PPRF was identified by its location with respect to the abducens nuclei (Strassman et al. 1986), the effects of stimulation (Cohen and Komatsuzaki 1972), and the discharge characteristics during head-restrained saccades (Keller 1974) and head-unrestrained gaze shifts (Whittington et al. 1984; Ling et al. 1999; Sylvestre and Cullen 2006). Stimulation was applied on penetrations that spanned anterior from the rostral pole of the abducens nucleus by 3.5 mm in one animal and 1.0 mm in the second. The distances covered along the medial-lateral extent spanned 1.25 mm in one and 2.5 mm in the other, with the midline lying roughly in the center of each range. Microstimulation was delivered mostly to the burst neuron region of the PPRF, although tracks penetrating through the abducens motoneurons were stimulated on occasion also. Furthermore, for several sites, stimulation of identical parameters was delivered in both head-restrained and head-unrestrained preparations.

On 20–33% of the trials, biphasic current pulses (0.25 ms pulse duration, 20–40 μA, 200–500 Hz, 200–500 ms) were delivered 100–200 ms into the gap period, and the yellow target was programmed to appear after stimulation offset. Stimulation parameters were selected on a site-by-site basis. We typically used the weakest parameters that both yielded a visually appreciable effect online and kept the animal engaged in the behavioral tasks. In a few cases, stimulation was delivered manually during the inter-trial interval. Furthermore, for some sites, the animal often produced a saccade that was superimposed on the stimulation-evoked movement. We believe these saccades were not produced by the stimulation because they did not occur on every trial, their onset times were quite variable, and their amplitudes and directions were random; such trials were removed from the analyses. Given these constraints and the need to preserve a sufficient number of trials to assess repeatability, our database was trimmed to include just the stimulation-evoked movements recorded from 21 sites. For

these trials, the eyes were within 12° of the center of the orbits and the head was pointing within 10° of straight-ahead location at stimulation onset.

Data were sampled at 500 Hz by an in-house acquisition program and analyzed off-line with Matlab, Statistica and customized software programs. Velocity criteria were used to detect the onset and offset of gaze, eye and head movements. For gaze and eye channels, the onset and offset velocity thresholds were 8 and 6°/s, respectively. For the head movement waveform, the onset and offset velocity thresholds were 5 and 3°/s, respectively. Every measurement was inspected visually and corrected manually if necessary. Gaze, eye and head *amplitudes* were computed as the displacements of position between the onset and offset of the respective waveforms. For all movements, head and eye *contributions* were defined as the respective changes in head and eye positions during the gaze shift. For visually-guided gaze shifts, the offset of the eye movement typically corresponds to the end of the saccadic eye movement. For PPRF stimulation-evoked movements, eye offset determined on the basis of a velocity criterion need not correspond to a meaningful event. Hence, the pertinent analyses employed eye contribution as a parameter.

Results

The effects of stimulation of the burst neuron region of the PPRF on eye and head signals were recorded from 21 sites (n = 16, monkey BE; (n = 5, monkey CH). For 4 of these sites (all from monkey BE) the data are limited to the condition when microstimulation was delivered during the inter-trial interval, when the animal was sitting in the dark. The results in the two configurations were similar and therefore pooled together. For 10 (n = 8, monkey BE; n = 2, monkey CH) of the 21 sites, the effects of matched stimulation parameters were investigated in both head-unrestrained and head-restrained conditions.

Microstimulation of PPRF

Amplitude and velocity traces of eye movements evoked by stimulation of the PPRF region in the head-restrained monkey are shown in Fig. 1. Each panel overlays several trials from a given site, and each column illustrates data from a different site. In agreement with previous reports (Cohen and Komatsuzaki 1972), constant-frequency stimulation evoked a relatively constant velocity eye movement (Fig. 1a–c). At other sites (n = 5), the stimulation initially produced a bell-shaped velocity profile that smoothly transitioned into a steady-state, constant velocity pattern (Fig. 1d). This waveform is distinct from that described previously (Cohen and Komatsuzaki 1972) as well as from that evoked by high-frequency and prolonged duration stimulation of the superior colliculus, which produces repeated patterns of the high velocity profiles interspersed with pursuit-like movement in between (Breznen et al. 1996; Missal et al. 1996; Moschovakis et al. 1998). Note that the changes in gaze and eye positions are equivalent because the head was held stationary.

When the head was allowed to move, constant-frequency stimulation produced nearly constant-velocity changes in the gaze, but not the eye, component of the gaze shift. In fact, an assortment of eye and head contribution patterns was observed across the stimulation sites. Panels e–h show amplitude and velocity profiles of gaze, head, and eye components evoked by stimulation of the same sites and with the same parameters as those highlighted in panels a–d. For the site illustrated in Fig. 1e the head contribution was significant, but it remained smaller than the change in gaze. The initial effect was similar for the site shown in Fig. 1f. However, with prolonged stimulation the head accelerated dramatically, such that head position led gaze position, and the eyes moved in the opposite direction in the orbits. For the site represented in Fig. 1g, the eyes and head began to rotate in opposite directions much earlier in the stimulation train, but the head did not display any high velocity movements. Stimulation of numerous sites (n = 8) also produced a transient, high velocity

change in gaze, which was followed by a constant velocity movement (Fig. 1h). Although the head movements associated with this example site appear negligible, this was not the case for all eight stimulation sites. Five of these 8 sites were also tested in the head-restrained condition (e.g, Fig. 1d), and similar velocity waveforms were observed for all sites. Overall, there was no systematic relationship between the location of the track along the anterior-posterior and medial-lateral axes, and the amount the head contributed to the gaze shift or the magnitude of the gaze shift.

For two sites, stimulation duration was systematically varied, because the animal continued to perform the behavioral tasks. Figure 2 shows stimulation-evoked movements obtained from one site for stimulation durations of 50, 100 and 200 ms; stimulation intensity (25 μA) and frequency (300 Hz) were held constant. For both head-unrestrained and head-restrained conditions, the gaze velocity reached a steady-state value of ~100°/s, and the gaze amplitude scaled linearly with stimulation duration. When the head was free to move, the change in gaze was produced as a coordinated movement of the eyes and head. Results from the second site were comparable.

Eye-head coordination

One way to quantify the eye-head coupling during the stimulation-evoked movements is to measure the contribution of each component associated with the stimulation-evoked change in gaze. Eye and head contributions are defined as the displacements in eye-in-head and head-in-space positions, respectively, during the period of the gaze shift. Figure 3 plots the eye (filled circles) and head (filled squares) contributions as a function of gaze shift amplitude for movements evoked by stimulation of the PPRF; each pair of symbols represents the average contribution for one stimulation site ($n = 21$). For comparison, the eye and head contributions associated with visually-guided gaze shifts are shown in the open gray circles and squares, respectively. As expected, for gaze shifts generated to orient to a visual target, eye and head contributions obey a lawful relationship (Freedman and Sparks 1997b): eye contribution increases linearly and then begins to saturate for gaze shifts greater than ~30°, whereas head contribution is negligible for small changes in line of sight and increases linearly for gaze shifts greater than ~20°. In contrast, the distributions of eye and head contributions measured in the movements evoked by stimulation of the PPRF do not obey this relationship. An obvious distinction is that eye contribution can be negative, highlighting the observation that the eyes and head can rotate in opposite directions during PPRF stimulation, even as gaze position shifts at a constant velocity in the ipsilateral direction.

Figure 3b provides another representation of the different characteristics shown by visually guided gaze shifts and PPRF stimulation-evoked movements. The illustration plots head contribution as a function of eye contribution for visually guided gaze shifts (○) and for movements evoked by stimulation of the PPRF (■). The two distributions are clearly different and nearly non-overlapping.

According to the data shown in Fig. 3, stimulation of some sites ($n = 5$) evoked gaze amplitudes executed as eye movements with minimal head contributions (<3°), although the head contribution for these sites ranged from 5 to 25% of gaze amplitude. Others ($n = 4$) produced large changes in head with a relatively small change in gaze (<6°), because the eyes counter-rotated substantially in the head; for these sites, head contribution ranged from 95 to 355% of the gaze shift. While we recognize that the exact distributions of eye and head contributions depend on the stimulation parameters, the fundamental difference in eye-head coordination between visually-guided and PPRF stimulation-evoked movements remains clear.

Figure 4a plots mean head latency as a function of mean gaze latency for the 21 stimulation sites tested with the head free to move. The mean ± SD gaze latency was 14.3 ± 7.9 ms (median: 13.3 ms; range: 3.6–37.7 ms) (Note that the 3.6 ms is less than the 4.8 ± 0.5 ms reported for midflight electrical stimulation of the PPRF (Miyashita and Hikosaka 1996). This difference is attributed to our low velocity threshold criterion and/or the visual inspection method in the previous study). In contrast, the head onset distribution was more variable. There were six sites (filled circles) for which head latency was >100 ms. These sites contained trials with very small head movements (Fig. 4b), making the detection of onset unreliable. Omission of these sites constrained the mean ±SD head latency to 63.6 ± 17.1 ms (median: 63.3 ms; range: 29.7–90.4 ms). Thus, head movement followed gaze onset by 49.6 ± 22.9 ms. In our database, there were no trials in which the head movement preceded gaze onset, presumably because the stimulation site was downstream of the omnipause neurons that gate the saccade pathway. For head-restrained data, gaze onset followed stimulation onset by 12.9 ± 3.6 ms (median: 13.0 ms; range: 6.8–17.6 ms) across the 10 sites. The gaze latency distributions from the head-restrained and head-unrestrained conditions were not significantly different from each other (two-tailed *t*-test, $P > 0.7$). In the head-restrained condition, gaze offset followed stimulation offset by 17.8 ± 7.9 ms (median: 15.5 ms; range: 10.0–31.4 ms) across the 10 sites. When the head was free to move, gaze offset lagged stimulation offset by 22.4 ± 8.8 ms (median: 20.6 ms; range: 7.1–31.7 ms). The offset of the head movement was more variable (mean ± SD: 64.9 ± 42.4 ms; median: 72.8 ms; range: 10.9–119.3 ms)), which is not unexpected given the different patterns of eye-head coordination evoked by the various stimulation sites.

Stimulation of the burst neuron region in the PPRF evoked primarily horizontal movements. The mean ±SD gaze direction in the head-restrained condition was 2.00 ± 5.26° (median: 3.27°; range: −7.7° to 11.8°), where 0° indicates a purely horizontal, ipsiversive movements. For the same 10 sites studied during the head-unrestrained condition, the mean ±SD gaze direction was −4.29 ± 7.71° (median: −3.14°; range: −22.5° to 3.7°). The two gaze direction distributions were not significantly different (Watson U^2 test, $P > 0.05$), although a nonparametric paired-sample comparison did reveal a statistical significance (Moore Test, $P < 0.001$) (Zar 1999). The head movement associated with stimulation-evoked gaze shift was also horizontal on average; the mean ± SD (median) direction was −2.38 ± 10.68° (median: −2.69°; range: −21.7° to 13.6°).

Ocular counter-rotation

The compensatory movement of the eyes evoked in response to a head movement is known as the vestibulo-ocular reflex (VOR). The VOR status during stimulation-evoked movements was assessed using two analyses. First, we compared the amplitudes of gaze shifts for the datasets in which identical stimulation parameters were administered in both head-restrained and head-unrestrained conditions (Fig. 5). These data were collected from 10 sites, but for two of these locations (gray and dark circles), multiple stimulation parameters were used in both modes. If the gain of the vestibular-ocular reflex (VOR) is indeed near unity during the head movements associated with the stimulation, then the gaze amplitude should be comparable in the two conditions. The slope of the linear regression is 1.05, the intercept is −0.35, and the correlation coefficient is 0.87 ($P < 0.0001$, two-tailed *t*-test). The mean ± SD of the ratio of corresponding gaze amplitudes in head-restrained and head-unrestrained conditions is 1.03 ± 0.25 (median: 1.03; range: 0.59–1.38), which is not significantly different from one ($P > 0.7$, two-tailed *t*-test).

The second approach was designed to provide a more thorough insight into the status of VOR gain. In conditions where the only input to the extraocular motoneurons is the vestibular consequence of a head-in-space rotation, such as during passive whole body rotation, the VOR gain is defined as $-\dot{E}/\dot{H}$, where $\dot{E}$ and $\dot{H}$ represent the observed eye and

head velocity waveforms, respectively (Leigh and Zee 1999). We believe that using the same computational rule is not appropriate when extra-vestibular signals, such as an oculomotor drive, also contribute to the output of extraocular motoneurons. During coordinated eye-head movements, the output of the extraocular motoneurons (MN_e) incorporates an excitatory drive from the saccadic system and an inhibitory input from the vestibular system (inset, Fig. 6c). The excitation provides an eye velocity command ($\dot{E}_{command}$) and the inhibition reflects a signal proportional to the head velocity ($\alpha\dot{H}$), where the proportionality constant (α) reflects the VOR gain. Thus, the observed eye-in-head velocity is defined as $\dot{E} = \dot{E}_{command} - \alpha\dot{H}$. It follows then that to compute the ocular compensation that occurs due to the head movement, the eye movement component generated by the excitatory drive must be subtracted from the observed eye velocity. In other words, the VOR gain should be calculated as $\alpha = -(\dot{E} - \dot{E}_{command})/\dot{H}$.

Computation of the VOR gain based on this formula requires an estimate of $\dot{E}_{command}$, which was derived from the eye movements evoked by PPRF stimulation in the head-restrained condition. Since head movements cannot be generated in this situation, $\dot{H} = 0$ and $\dot{E} = \dot{E}_{command}$. Thus, we used the steady-state value of the constant-velocity eye movements evoked by stimulation of the PPRF (Fig. 1) for an estimate of the eye velocity command. We assume that stimulation of the same site with identical parameters in the head-unrestrained condition delivers an identical command to the extraocular motoneurons, and differences observed in the eye-in-head velocity in the two conditions are due to vestibular inputs (Similar reasoning was used to compute VOR gain during gaze shifts evoked by stimulation of the SC in the head-restrained and –unrestrained cat (Roucoux et al. 1980)).

To illustrate an example, Fig. 6a, b shows position and velocity waveforms of gaze, head and eye-in-head components of a single stimulation-evoked movement. Figure 6c plots the VOR gain computed as $-(\dot{E} - \dot{E}_{command})/\dot{H}$. Note that VOR gain was computed once the head movement had initiated. The cyan trace illustrates the calculated VOR gain for the duration starting from head movement onset to stimulation offset (~410 ms for the illustrated trial), indicated by the thick traces. For this epoch, $\dot{E}_{command}$ was set to the steady-state velocity estimated from the head-restrained data. For the period ensuing stimulation offset (magenta trace in panel C), $\dot{E}_{command}$ was set to zero and the equation of VOR gain simplified to the traditional definition, $-\dot{E}/\dot{H}$. The computed VOR gain is transiently high at the onset of the head movement, presumably a consequence of division by a small head velocity value. The analysis indicates that the VOR gain hovers around unity for most of the stimulation duration and the period following stimulation offset. A brief discontinuity is also observed at the transition from cyan to magenta color due to instantaneous change in $\dot{E}_{command}$

To obtain a numerical value for the VOR gain, $(\dot{E} - \dot{E}_{command})$ was plotted as a function of $\dot{H}$ for the period shown as thick traces (approximately 300 ms for this trial; >100 ms for most trials) and a linear regression was applied to the data. Figure 7a (left) plots for all 125 trials from 10 stimulation sites a histogram of the VOR gain, which equals the negative of the slope of the best fit line. Table 1 summarizes this information by site. The mean ± SD counter-rotation gain across these trials was 1.03 ± 1.00, which is not significantly different from one (*t*-test, $P > 0.05$). The large variance in the gain is partly due to trials with small head contributions (Fig. 7a, right). When only considering trials with head contribution >3°, the mean ± SD and median counter-rotation gains were 1.14 ± 0.53 and 1.07, respectively ($n = 69$ trials). When only considering trials with head contribution >5°, the mean ± SD and median counter-rotation gains were 1.09 ± 0.42 and 1.07, respectively ($n = 48$ trials). In both cases, the mean gain was not significantly different from one (*t*-test, $P > 0.05$).

Figure 7b shows the distribution of the correlation coefficients of the individual linear regressions. Trials with small head contributions were typically associated with coefficients closer to zero, while trials with large head contributions had correlation coefficient approaching −1. Thus, when the PPRF stimulation evoked a sizeable head movement, the VOR gain hovered around unity and this was a robust observation. When the stimulation produced a small head movement, the counter-rotation gain tended to be more variable, as was our confidence in the statistical significance of the fits.

Microstimulation of extraocular motoneurons

Stimulation of the ipsilateral abducens nucleus in the head-unrestrained animal (Fig. 8a) guided the gaze position to an eccentric, ipsilateral location with an exponential time course. Once the stimulation was terminated, gaze retreated, also exponentially, towards the initial position. The change in gaze was produced almost exclusively by the eye. The head contribution was negligible and, if detected, its onset occurred late in the trial, typically after the eyes reached eccentric locations in the orbits; thus, the head movement could have occurred due to modulation of neck muscle activity by eye positions in orbits (Vidal et al. 1982; Andre-Deshays et al. 1988; Corneil et al. 2002). When the head was restrained from moving (Fig. 8b), the change in gaze strikingly resembled the eye-in-head position waveforms observed in the head-unrestrained condition. For 9 sites ($n = 3$, monkey BE; $n = 6$, monkey CH) we compared the stimulation-evoked change in gaze in the head-restrained and head-unrestrained conditions. For identical stimulation parameters, the mean ± SD ratio of gaze amplitudes (head-unrestrained/head-restrained) was 1.09 ± 0.27 (median: 1.03), which was not significantly different from one (two-tailed t-test, $P > 0.3$). Thus the primary effect of stimulation of extraocular motoneurons was to exponentially drive the eye only to an eccentric location in the orbit.

Discussion

The role of PPRF neurons in the control of coordinated eye-head movements was addressed using microstimulation techniques. Biphasic current pulses of constant amplitude and frequency were delivered where neurons that discharge high frequency bursts during gaze shifts were encountered. In the head-unrestrained monkey, the stimulation evoked a relatively constant velocity change in gaze using combinations of eye and head movements. Though the eye-head coordination was consistent within a site, the pattern was unpredictable on a site-by-site basis (Fig. 1). Unlike what is observed for gaze shifts oriented to a visual target (Freedman and Sparks 1997b; Gandhi and Sparks 2001), there was no systematic change in eye and head contributions as a function of gaze amplitude (Fig. 3). For a subset of sites, stimulation of identical parameters was also delivered to the PPRF region in the head-restrained condition. As reported previously (Cohen and Komatsuzaki 1972), the stimulation evoked a constant velocity change in eye position (Fig. 1a–d). Interestingly, the changes in gaze were comparable for the head-restrained and head-unrestrained conditions, suggesting that the VOR gain was near unity during the stimulation-evoked eye-head movements (Figs. 5, 6, 7). For comparison, microstimulation was also delivered to the extraocular motoneurons (Fig. 8). The stimulation induced an exponential change in gaze produced predominantly by the eye (Reinhart and Zuber 1970; Sklavos et al. 2002), and the head movement was negligible when the head was unrestrained. Following stimulation offset, gaze retreated exponentially towards the initial position, although its return was usually interrupted by a spontaneous gaze shift.

Effectors controlled by PPRF neurons

What do the data obtained when stimulating the PPRF burst neuron region imply about the effectors controlled by these cells? The participation of neurons with saccade-related bursts

in the control of eye movements is well documented (see Sparks 2002 for a review). At least a subset of these cells, excitatory burst neurons (EBNs), projects directly to the ipsilateral abducens nucleus (Strassman et al. 1986) and discharges a number of spikes directly proportional to the amplitude of the horizontal component of a saccade (Keller 1974). The eye movement evoked by stimulation of the PPRF region in the head-restrained monkey is consistent with EBN activity: for a fixed current intensity and frequency, the amplitude of the movement is proportional to the number of stimulation pulses (Cohen and Komatsuzaki 1972). In contrast, the role of pontine burst cells in the control of coordinated eye-head movement is controversial (Sparks 1999; Sparks and Gandhi 2003). When the head is unrestrained, the number of spikes is directly proportional to gaze amplitude, not its ocular component (Ling et al. 1999), and the temporal waveform of the neural activity is best modeled as a function of eye and head velocities (based on an extension of the Cullen and Guitton (1997) study on IBNs, which are the inhibitory counterpart of EBNs). However, if the VOR gain during the gaze shift is greater than zero (it doesn't have to be one), the vestibular system imposes an inhibition command that counteracts a portion of the excitatory, saccadic drive on the abducens motoneurons (see inset, Fig. 6c). Consequently, the executed ocular component will not correlate strongly with the pontine burst neuron activity, and the observed eye movement will not match the motor command that was issued for the eye component of the gaze shift (Cullen and Guitton 1997; Ling et al. 1999; Sparks 1999; Sparks and Gandhi 2003).

In the present study, a microstimulation approach was used to gain additional insight regarding the role of the PPRF region in the control of head movements. One consistent finding was the similarity in gaze velocity profiles for both head-restrained and head-unrestrained conditions for any given site. We do *not* interpret this result to suggest that the PPRF region encodes gaze movement commands because the eye and head components of the change in gaze were not systematic across sites; i.e., a variety of effects were noted, ranging from eye-only to combined eye-head to predominantly head-only movements (Fig. 1e–h). These observations imply that stimulation of some sites activated neurons that participate in eye movement control *only*, whereas stimulation of other sites also activated cell bodies and/or fibers of passage that contribute to head movement control (see below). Unfortunately, confounds introduced by the likely activation of passing fibers that relay information to the neck motoneurons prevents any firm conclusions. In fact, one interpretation that cannot be rejected is the traditional and parsimonious view that a subset of neurons, perhaps the EBNs, relays motor commands to the extraocular motoneurons *only*. Results of several previous studies are consistent with this hypothesis. During large head-unrestrained gaze shifts, stimulation of omnipause neurons, which inhibit EBNs, interrupts primarily the ocular component of gaze shifts (Gandhi and Sparks 2007). In fact, a head movement without an accompanying gaze shift is typically initiated during prolonged stimulation of the omnipause neurons prior to gaze onset (Gandhi and Sparks 2007). Also, intra-axonal injections of physiologically characterized EBNs in the squirrel monkey did not reveal axons that extend beyond the prepositus (Strassman et al. 1986), although a poly-synaptic connection cannot be excluded. Finally, some component of the observed head movement could have resulted from modulation of neck muscle activity as the eyes were driven to increasingly ipsilateral positions in the orbits (Vidal et al. 1982; Andre-Deshays et al. 1988; Corneil et al. 2002; Wang et al. 2007).

If not the EBNs, then what neural elements mediate the head movements evoked by stimulation of some PPRF sites? One possibility is that stimulation recruited fibers that traverse through the PPRF region and relay projections to the neck motoneurons (e.g., May and Porter 1992; Warren et al. 2008). Another candidate is a subset of reticulospinal neurons that reside in the PPRF region (Grantyn et al. 1987; Iwamoto and Sasaki 1990; Iwamoto et al. 1990; Robinson et al. 1994). Scudder et al. (2002) proposed that long-lead burst neurons

(LLBNs), which are intermingled with the EBNs, may be involved in controlling both eye and head movements. Intra-axonal injection of LLBNs revealed projections toward the spinal cord in the squirrel monkey (Scudder et al. 1996) and also to the abducens nucleus in the cat (Grantyn and Berthoz 1987; Grantyn et al. 1987). The discharge characteristics of LLBNs is not temporally constrained to the duration of the gaze shift. In fact, many LLBNs continue to discharge until the end of the head movement, well beyond the end of the gaze shift (Phillips et al. 2001). Neurons in the medullary reticular formation in the cat also exhibit similar discharge characteristics (Isa and Naito 1995).

Status of the VOR gain: comparison with previous studies

Two different analyses—comparison of gaze amplitude in the head-restrained and head-unrestraind conditions (Fig. 5) and accounting for the oculomotor input to the abducens nucleus (Figs. 6, 7; Table 1)—were used to evaluate the VOR gain. Both approaches suggest that the gain is near unity during movements evoked by PPRF stimulation. In contrast to the PPRF data, stimulation of certain regions of the nucleus reticularis gigantocellularis (NRG) produces movements (Sprague and Chambers 1954; Cowie and Robinson 1994; Quessy and Freedman 2004; Sasaki et al. 2004) with an attenuated VOR gain (Quessy and Freedman 2004). The NRG resides caudal to the abducens nucleus (Peterson et al. 1975; Tohyama et al. 1979; Huerta and Harting 1982; Cowie et al. 1994; Robinson et al. 1994) and, compared to the PPRF, has a higher density of projections to the neck motoneurons (Tohyama et al. 1979; Grantyn and Berthoz 1988). Quessy and Freedman (2004) assumed that they activated neurons within the pathway controlling only head movements and, therefore, interpreted the observed eye movement as VOR gain readout. They noted a counter-rotation gain of <0.4, which contrasts with the near unity gain we noted during PPRF stimulation. While we don't have a solid explanation for the discrepancy, we entertain the possibility that stimulation of the NRG activated— antidromically, orthodromically or via current spread— neural circuits in the oculomotor pathway in addition to recruiting elements in the head pathway.

Roucoux et al. (1980) stimulated the feline superior colliculus in head-restrained and head-unrestrained conditions. Using analysis like that represented in Fig. 7, they showed that the VOR gain varies dynamically and is dependent on the site of stimulation within the colliculus. The gain was near unity for stimulation of the anterior zone but substantially suppressed, even negative, when stimulation was applied in the intermediate zone, which evoked large amplitude gaze shifts. Their results are more in line with the accepted notion that the VOR gain is dynamically attenuated during visually-guided gaze shifts (Laurutis and Robinson 1986; Pélisson and Prablanc 1986; Tomlinson and Bahra 1986; Guitton and Volle 1987; Pélisson et al. 1988; Lefèvre et al. 1992; Tabak et al. 1996; Roy and Cullen 1998, 2002; Cullen et al. 2004). How can this discrepancy be resolved? Noting the obvious differences in the kinematics of the visually-guided and PPRF stimulation-evoked movements, it is apparent that the stimulation recruited only a subset of the neural circuitry activated during large gaze shifts to eccentric targets. For example, generation of a horizontal orienting movement to an object presented in the visual periphery excites saccade-related burst neurons in cortical and subcortical oculomotor structures; requires a spatiotemporal transformation that activates a population of neurons in the pontomedullary reticular formation (including the EBNs and LLBNs), cerebellum, and cervical spinal cord; performs a decomposition computation of desired gaze shift into desired eye and head components; and induces an inhibition of OPNs in PPRF to trigger the gaze shift. Stimulation of the PPRF, in contrast, may not activate cortical regions or the superior colliculus in a normal manner, if at all, and therefore may not necessitate a spatiotemporal transformation; the EBNs and LLBNs activated by the stimulation are probably only a fraction of the population recruited during visually-guided movements; and the OPNs may not be inhibited. These factors are likely to yield movements with slower gaze kinematics.

Furthermore, the circuit that gates or attenuates the VOR may not be activated during the PPRF stimulation. In essence, the head movements produced by PPRF stimulation may be treated as passive head movements and, therefore, processed differently from active head movements associated with gaze shifts (Cullen and Roy 2004). Thus, the default VOR state (gain of unity) persists during the eye-head movements evoked by PPRF stimulation.

Acknowledgments

We thank Dennis Murray for surgical assistance and animal care, and Kathy Pearson for software development. The study was funded by NIH grants EY001189, EY007001, EY007009 and EY015485.

References

Andre-Deshays C, Berthoz A, Revel M. Eye-head coupling in humans. I. Simultaneous recording of isolated motor units in dorsal neck muscles and horizontal eye movements. Exp Brain Res. 1988; 69:399–406. [PubMed: 3345816]

Breznen B, Lu SM, Gnadt JW. Analysis of the step response of the saccadic feedback: system behavior. Exp Brain Res. 1996; 111:337–344. [PubMed: 8911928]

Chen LL, Walton MM. Head movement evoked by electrical stimulation in the supplementary eye field of the rhesus monkey. J Neurophysiol. 2005; 94:4502–4519. [PubMed: 16148273]

Cohen B, Komatsuzaki A. Eye movements induced by stimulation of the pontine reticular formation: evidence for integration in oculomotor pathways. Exp Neurol. 1972; 36:101–117. [PubMed: 4558412]

Corneil BD, Olivier E, Munoz DP. Neck muscle activity evoked by stimulation of the monkey superior colliculus. I. Topography and manipulation of stimulation parameters. J Neurophysiol. 2002; 88:1980–1999. [PubMed: 12364523]

Cowie RJ, Robinson DL. Subcortical contributions to head movements in macaques. I. Contrasting effects of electrical stimulation of a medial pontomedullary region and the superior colliculus. J Neurophysiol. 1994; 72:2648–2664. [PubMed: 7897481]

Cowie RJ, Smith MK, Robinson DL. Subcortical contributions to head movements in macaques. II. Connections of a medial pontomedullary head-movement region. J Neurophysiol. 1994; 72:2665–2682. [PubMed: 7534824]

Cullen KE, Guitton D. Analysis of primate IBN spike trains using system identification techniques. II. Relationship to gaze, eye, and head movement dynamics during head-free gaze shifts. J Neurophysiol. 1997; 78:3283–3306. [PubMed: 9405545]

Cullen KE, Roy JE. Signal processing in the vestibular system during active versus passive head movements. J Neurophysiol. 2004; 91:1919–1933. [PubMed: 15069088]

Cullen KE, Huterer M, Braidwood DA, Sylvestre PA. Time course of vestibuloocular reflex suppression during gaze shifts. J Neurophysiol. 2004; 92:3408–3422. [PubMed: 15212424]

Freedman EG, Sparks DL. Activity of cells in the deeper layers of the superior colliculus of the rhesus monkey: evidence for a gaze displacement command. J Neurophysiol. 1997a; 78:1669–1690. [PubMed: 9310452]

Freedman EG, Sparks DL. Eye-head coordination during head-unrestrained gaze shifts in rhesus monkeys. J Neurophysiol. 1997b; 77:2328–2348. [PubMed: 9163361]

Freedman EG, Stanford TR, Sparks DL. Combined eye-head gaze shifts produced by electrical stimulation of the superior colliculus in rhesus monkeys. J Neurophysiol. 1996; 76:927–952. [PubMed: 8871209]

Gandhi NJ, Sparks DL. Microstimulation of the pontine reticular formation in monkey: effects on coordinated eye-head movements. Soc Neurosci. 2000 Abstr 109.8.

Gandhi NJ, Sparks DL. Experimental control of eye and head positions prior to head-unrestrained gaze shifts in monkey. Vision Res. 2001; 41:3243–3254. [PubMed: 11718770]

Gandhi NJ, Sparks DL. Dissociation of eye and head components of gaze shifts by stimulation of the omnipause neuron region. J Neurophysiol. 2007; 98:360–373. [PubMed: 17493925]

Grantyn A, Berthoz A. Reticulo-spinal neurons participating in the control of synergic eye and head movements during orienting in the cat. I. Behavioral properties. Exp Brain Res. 1987; 66:339–354. [PubMed: 3595779]

Grantyn, A.; Berthoz, A. The role of the tectoreticulospinal system in the control of head movement. In: Peterson, BW.; Richmond, FJ., editors. Control of head movement. New York: Oxford University Press; 1988. p. 224-244.

Grantyn A, Ong-Meang Jacques V, Berthoz A. Reticulo-spinal neurons participating in the control of synergic eye and head movements during orienting in the cat. II. Morphological properties as revealed by intra-axonal injections of horseradish peroxidase. Exp Brain Res. 1987; 66:355–377. [PubMed: 3595780]

Guitton D, Volle M. Gaze control in humans: eye-head coordination during orienting movements to targets within and beyond the oculomotor range. J Neurophysiol. 1987; 58:427–459. [PubMed: 3655876]

Guitton D, Crommelinck M, Roucoux A. Stimulation of the superior colliculus in the alert cat. I. Eye movements and neck EMG activity evoked when the head is restrained. Exp Brain Res. 1980; 39:63–73. [PubMed: 7379886]

Huerta MF, Harting JK. Tectal control of spinal cord activity: neuroanatomical demonstration of pathways connecting the superior colliculus with the cervical spinal cord grey. Prog Brain Res. 1982; 57:293–328. [PubMed: 6296921]

Isa T, Naito K. Activity of neurons in the medial pontomedullary reticular formation during orienting movements in alert head-free cats. J Neurophysiol. 1995; 74:73–95. [PubMed: 7472355]

Iwamoto Y, Sasaki S. Monosynaptic excitatory connections of reticulospinal neurones in the nucleus reticularis pontis caudalis with dorsal neck motoneurones in the cat. Exp Brain Res. 1990; 80:277–289. [PubMed: 2358043]

Iwamoto Y, Sasaki S, Suzuki I. Input-output organization of reticulospinal neurones, with special reference to connections with dorsal neck motoneurones in the cat. Exp Brain Res. 1990; 80:260–276. [PubMed: 2358042]

Keller EL. Participation of medial pontine reticular formation in eye movement generation in monkey. J Neurophysiol. 1974; 37:316–332. [PubMed: 4205567]

Klier EM, Wang H, Crawford JD. The superior colliculus encodes gaze commands in retinal coordinates. Nat Neurosci. 2001; 4:627–632. [PubMed: 11369944]

Knight TA, Fuchs AF. Contribution of the frontal eye field to gaze shifts in the head-unrestrained monkey: effects of microstimulation. J Neurophysiol. 2007; 97:618–634. [PubMed: 17065243]

Laurutis VP, Robinson DA. The vestibulo-ocular reflex during human saccadic eye movements. J Physiol Lond. 1986; 373:209–233. [PubMed: 3489091]

Lefèvre P, Bottemanne I, Roucoux A. Experimental study and modeling of vestibulo-ocular reflex modulation during large shifts of gaze in humans. Exp Brain Res. 1992; 91:496–508. [PubMed: 1483522]

Leigh, RJ.; Zee, DS. The neurology of eye movements. New York: Oxford University Press; 1999.

Ling L, Fuchs AF, Phillips JO, Freedman EG. Apparent dissociation between saccadic eye movements and the firing patterns of premotor neurons and motoneurons. J Neurophysiol. 1999; 82:2808–2811. [PubMed: 10561447]

Martinez-Trujillo JC, Wang H, Crawford DJ. Electrical stimulation of the supplementary eye fields in the head-free macaque evokes kinematically normal gaze shifts. J Neurophysiol. 2003; 89:2961–2974. [PubMed: 12611991]

May PJ, Porter JD. The laminar distribution of macaque tectobulbar and tectospinal neurons. Vis Neurosci. 1992; 8:257–276. [PubMed: 1372175]

Missal M, Lefèvre P, Delinte A, Crommelinck M, Roucoux A. Smooth eye movements evoked by electrical stimulation of the cat's superior colliculus. Exp Brain Res. 1996; 107:382–390. [PubMed: 8821380]

Miyashita N, Hikosaka O. Minimal synaptic delay in the saccadic output pathway of the superior colliculus studied in awake monkey. Exp Brain Res. 1996; 112:187–196. [PubMed: 8951387]

Moschovakis AK, Dalezios Y, Petit J, Grantyn AA. New mechanism that accounts for position sensitivity of saccades evoked in response to stimulation of superior colliculus. J Neurophysiol. 1998; 80:3373–3379. [PubMed: 9862936]

Munoz DP, Guitton D, Pélisson D. Control of orienting gaze shifts by the tectoreticulospinal system in the head-free cat. III. Spatiotemporal characteristics of phasic motor discharges. J Neurophysiol. 1991; 66:1642–1666. [PubMed: 1765799]

Paré M, Crommelinck M, Guitton D. Gaze shifts evoked by stimulation of the superior colliculus in the head-free cat conform to the motor map but also depend on stimulus strength and fixation activity. Exp Brain Res. 1994; 101:123–139. [PubMed: 7843291]

Pélisson D, Prablanc C. Vestibulo-ocular reflex (VOR) induced by passive head rotation and goal-directed saccadic eye movements do not simply add in man. Brain Res. 1986; 380:397–400. [PubMed: 3489503]

Pélisson D, Prablanc C, Urquizar C. Vestibuloocular reflex inhibition and gaze saccade control characteristics during eye-head orientation in humans. J Neurophysiol. 1988; 59:997–1013. [PubMed: 3367207]

Peterson BW, Maunz RA, Pitts NG, Mackel RG. Patterns of projection and branching of reticulospinal neurons. Exp Brain Res. 1975; 23:333–351. [PubMed: 1183508]

Phillips JO, Ling L, Fuchs AF. A comparison of excitatory and inhibitory burst neuron activity during active head-unrestrained gaze shifts. Soc Neurosci. 2001 Abstr 405.10.

Quessy S, Freedman EG. Electrical stimulation of rhesus monkey nucleus reticularis gigantocellularis. I. Characteristics of evoked head movements. Exp Brain Res. 2004; 156:342–356. [PubMed: 14985893]

Reinhart RJ, Zuber BL. Horizontal eye movements from abducens nerve stimulation in the cat. IEEE Trans Biomed Eng. 1970; 17:11–14. [PubMed: 5441213]

Robinson DA. Eye movements evoked by collicular stimulation in the alert monkey. Vision Res. 1972; 12:1795–1808. [PubMed: 4627952]

Robinson FR, Phillips JO, Fuchs AF. Coordination of gaze shifts in primates: brainstem inputs to neck and extraocular motoneuron pools. J Comp Neurol. 1994; 346:43–62. [PubMed: 7962711]

Roucoux A, Guitton D, Crommelinck M. Stimulation of the superior colliculus in the alert cat. II. Eye and head movements evoked when the head is unrestrained. Exp Brain Res. 1980; 39:75–85. [PubMed: 7379887]

Roy JE, Cullen KE. A neural correlate for vestibulo-ocular reflex suppression during voluntary eye-head gaze shifts. Nat Neurosci. 1998; 1:404–410. [PubMed: 10196531]

Roy JE, Cullen KE. Vestibuloocular reflex signal modulation during voluntary and passive head movements. J Neurophysiol. 2002; 87:2337–2357. [PubMed: 11976372]

Sasaki S, Yoshimura K, Naito K. The neural control of orienting: role of multiple-branching reticulospinal neurons. Prog Brain Res. 2004; 143:383–389. [PubMed: 14653181]

Schiller PH. The discharge characteristics of single units in the oculomotor and abducens nuclei of the unanesthetized monkey. Exp Brain Res. 1970; 10:347–362. [PubMed: 4987208]

Schiller PH, Stryker M. Single-unit recording and stimulation in superior colliculus of the alert rhesus monkey. J Neurophysiol. 1972; 35:915–924. [PubMed: 4631839]

Scudder CA, Moschovakis AK, Karabelas AB, Highstein SM. Anatomy and physiology of saccadic long-lead burst neurons recorded in the alert squirrel monkey. II. Pontine neurons. J Neurophysiol. 1996; 76:353–370. [PubMed: 8836230]

Scudder CA, Kaneko CS, Fuchs AF. The brainstem burst generator for saccadic eye movements: A modern synthesis. Exp Brain Res. 2002; 142:439–462. [PubMed: 11845241]

Sklavos SG, Gandhi NJ, Sparks DL, Porrill J, Dean P. Mechanics of oculomotor plant estimated from effects of abducens microstimulation. Soc Neurosci. 2002 Abstr 463.5.

Sparks DL. Conceptual issues related to the role of the superior colliculus in the control of gaze. Curr Opin Neurobiol. 1999; 9:698–707. [PubMed: 10607648]

Sparks DL. The brainstem control of saccadic eye movements. Nat Rev Neurosci. 2002; 3:952–964. [PubMed: 12461552]

Sparks DL, Gandhi NJ. Single cell signals: an oculomotor perspective. Prog Brain Res. 2003; 142:35–53. [PubMed: 12693253]

Sparks DL, Freedman EG, Chen LL, Gandhi NJ. Cortical and subcortical contributions to coordinated eye and head movements. Vision Res. 2001; 41:3295–3305. [PubMed: 11718774]

Sprague JM, Chambers WW. Control of posture by reticular formation and cerebellum in the intact, anesthetized and unanesthetized and in the decerebrated cat. Am J Physiol. 1954; 176:52–64. [PubMed: 13124495]

Stanford TR, Freedman EG, Sparks DL. Site and parameters of microstimulation: evidence for independent effects on the properties of saccades evoked from the primate superior colliculus. J Neurophysiol. 1996; 76:3360–3381. [PubMed: 8930279]

Strassman A, Highstein SM, McCrea RA. Anatomy and physiology of saccadic burst neurons in the alert squirrel monkey. I. Excitatory burst neurons. J Comp Neurol. 1986; 249:337–357. [PubMed: 3734160]

Sylvestre PA, Cullen KE. Premotor correlates of integrated feedback control for eye-head gaze shifts. J Neurosci. 2006; 26:4922–4929. [PubMed: 16672667]

Tabak S, Smeets JB, Collewijn H. Modulation of the human vestibuloocular reflex during saccades: probing by high-frequency oscillation and torque pulses of the head. J Neurophysiol. 1996; 76:3249–3263. [PubMed: 8930270]

Tohyama M, Sakai K, Salvert D, Touret M, Jouvet M. Spinal projections from the lower brain stem in the cat as demonstrated by the horseradish peroxidase technique. I. Origins of the reticulospinal tracts and their funicular trajectories. Brain Res. 1979; 173:383–403. [PubMed: 487101]

Tomlinson RD, Bahra PS. Combined eye-head gaze shifts in the primate. II. Interactions between saccades and the vestibuloocular reflex. J Neurophysiol. 1986; 56:1558–1570. [PubMed: 3806182]

Tu TA, Keating EG. Electrical stimulation of the frontal eye field in a monkey produces combined eye and head movements. J Neurophysiol. 2000; 84:1103–1106. [PubMed: 10938333]

Van Gisbergen JA, Robinson DA, Gielen S. A quantitative analysis of generation of saccadic eye movements by burst neurons. J Neurophysiol. 1981; 45:417–442. [PubMed: 7218009]

Vidal PP, Roucoux A, Berthoz A. Horizontal eye position-related activity in neck muscles of the alert cat. Exp Brain Res. 1982; 46:448–453. [PubMed: 6980136]

Wang X, Zhang M, Cohen IS, Goldberg ME. The proprioceptive representation of eye position in monkey primary somatosensory cortex. Nat Neurosci. 2007; 10:640–646. [PubMed: 17396123]

Warren S, Waitzman DM, May PJ. Anatomical evidence for interconnections between the central mesencephalic reticular formation and cervical spinal cord in the cat and macaque. Anat Rec. 2008; 291:141–160.

Whittington DA, Lestienne F, Bizzi E. Behavior of preoculomotor burst neurons during eye-head coordination. Exp Brain Res. 1984; 55:215–222. [PubMed: 6745362]

Zar, JH. Biostatistical analysis. Upper Saddle River, NJ: Prentice-Hall; 1999.

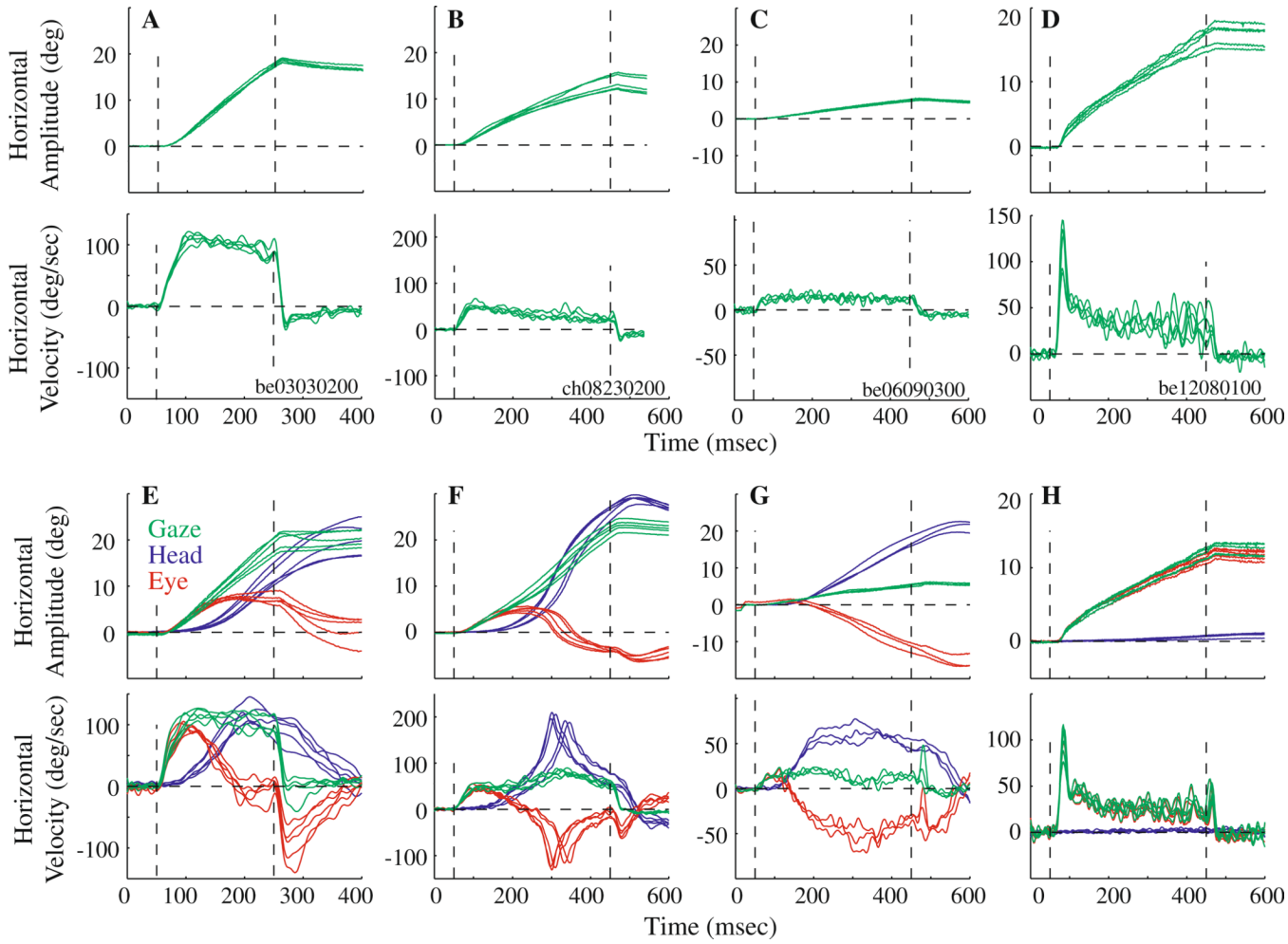

Fig. 1.

Effects of microstimulation of the PPRF region in monkey. **a–d** Stimulation delivered with the head immobilized. Each panel superimposes several traces (n = 4–5) of horizontal amplitude (*top*) and velocity (*bottom*) waveforms of stimulation-evoked movements from four different sites. Stimulation parameters: **a** 25 μA, 200 ms, 300 Hz; **b** 20 μA, 400 ms, 300 Hz; **c** 25 μA, 400 ms, 300 Hz; **d** 20 μA, 400 ms, 400 Hz. *Vertical dashed lines* indicate stimulation onset and offset, and *horizontal dashed lines* mark zero displacement and velocity. The initial position was subtracted from each trace to align the movements. **e–h** Stimulation delivered with the head unrestrained. Each panel superimposes representative stimulation-evoked movements (n = 3–7) evoked from the same four sites and using the same parameters as above. *Top and bottom panels* plot horizontal components of representative stimulation-evoked changes in amplitude and velocity, respectively, of gaze (*green*), head-in-space (*blue*), and eye-in-head (*red*)

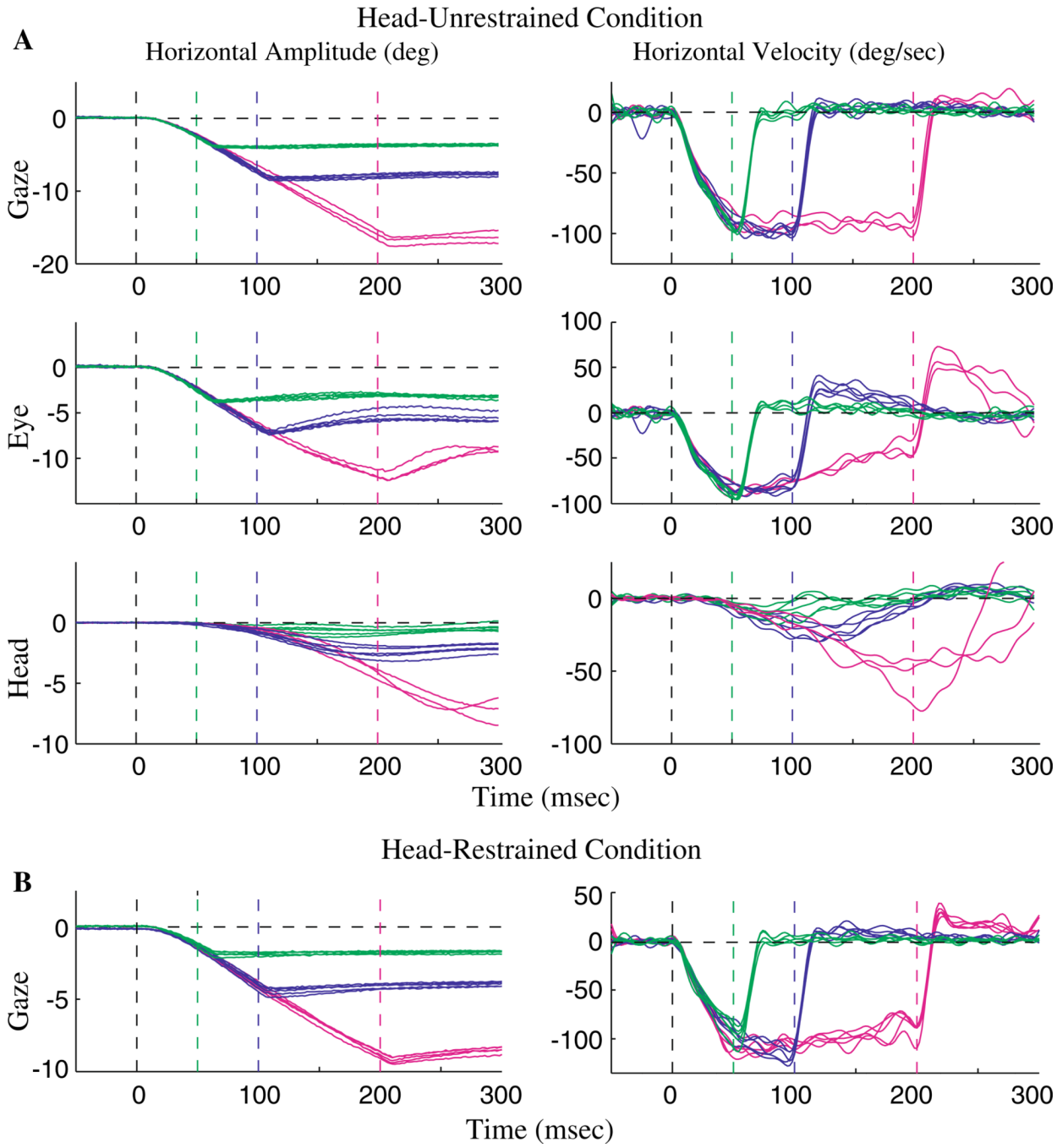

Fig. 2.

Effects of varying stimulation duration on eye-head movements evoked by stimulation of the PPRF region. **a** Head-unrestrained condition. The *green, blue*, and *magenta* traces show movements when stimulation duration was set to 50, 100, and 200 ms, respectively. Stimulation intensity (25 μA) and frequency (300 Hz) were held constant. The individual rows plot horizontal gaze, eye-in-head and head amplitude (*left column*) and velocity (*right column*) for representative, individual trials. The first vertical line marks stimulation onset, and the remaining vertical lines denote stimulation offset for the three different durations (indicated by the different colors). **b** Head-restrained condition. The same format as above,

but only the gaze channel is shown as the head was held stationary. Thus, the eye component equals the gaze component

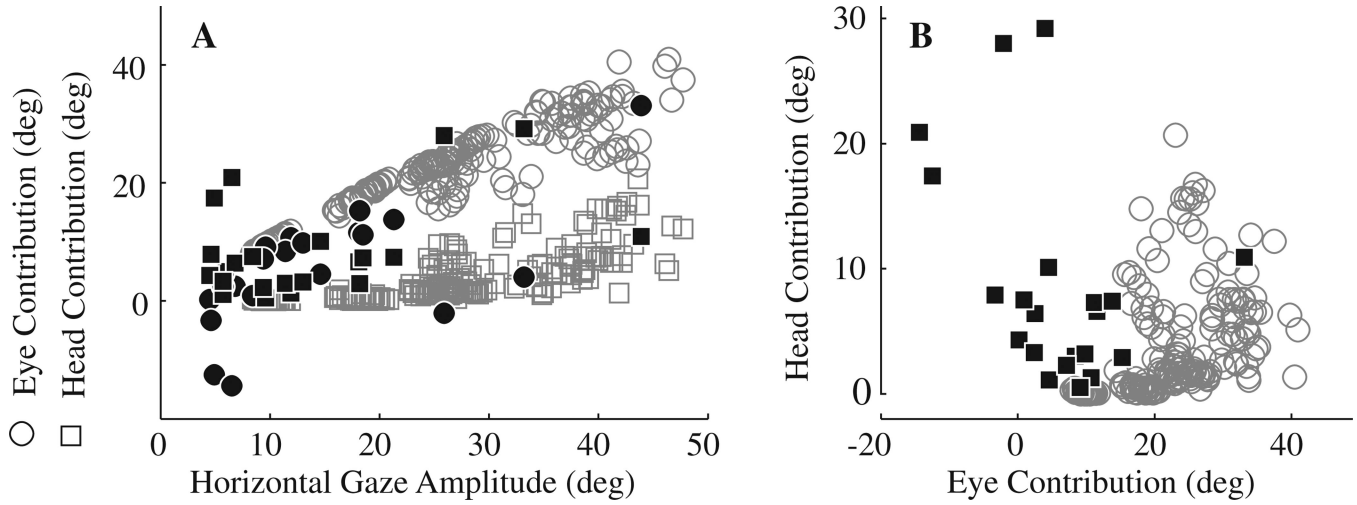

Fig. 3.

Distribution of eye and head contributions. **a** Eye (○) and head (□) contributions are plotted as a function of horizontal gaze amplitude evoked by stimulation of the PPRF region (*filled symbols; n* = 21 sites) and for visually-guided, horizontal gaze shifts (*open, gray symbols; n* = 200). Note that eye contributions can be negative for positive, stimulation-evoked changes in gaze (e.g., Fig. 1f, g). For the visually-guided gaze shifts, the initial eye positions were limited to ±5° and initial head positions were restricted to ±10°. For the stimulation-evoked movements, the initial eye positions were limited to ±12° and initial head positions were restricted to ±10°. **b** An alternate representation of panel **a**. Head contribution is plotted as function of eye contribution for visually-guided gaze shifts (○) and for eye-head movement evoked by stimulation of the PPRF (■). The distributions of two types of movements are clearly different

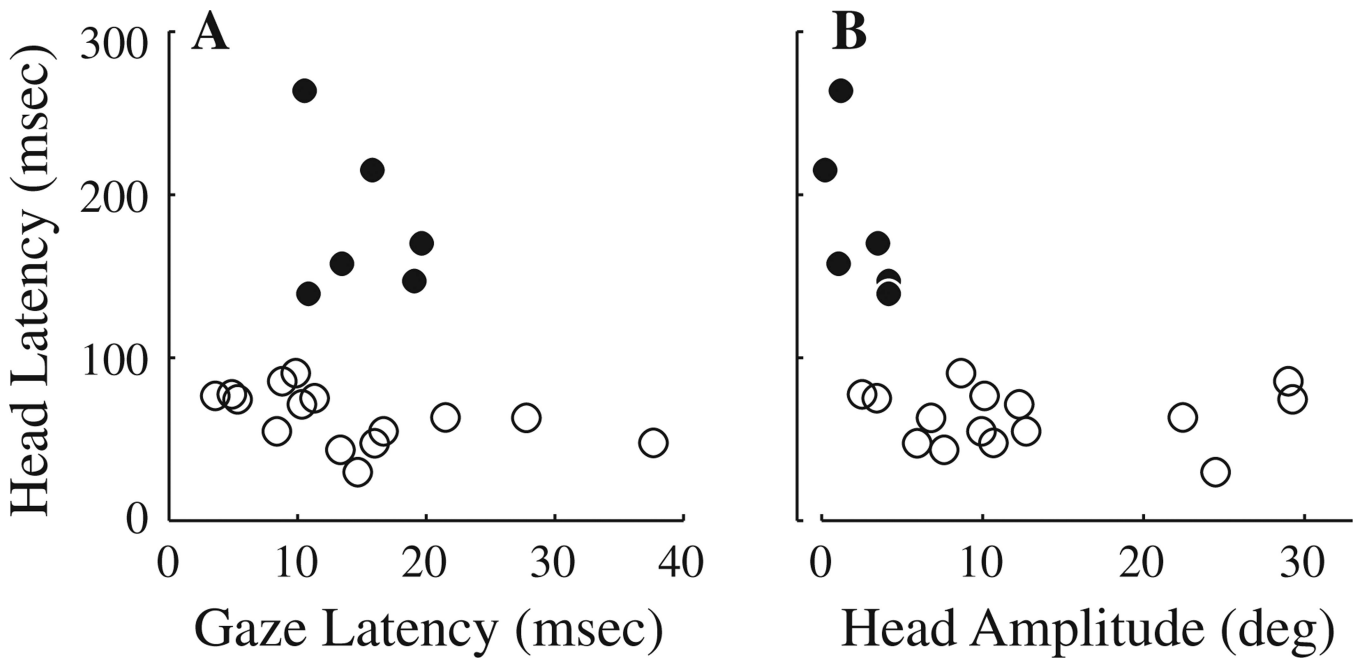

Fig. 4.

Analyses of the latency of stimulation-evoked movements. a Head latency is plotted against gaze latency. Apart from the six sites for which head latency was prolonged (●), head onset followed gaze onset by 49.6 ± 22.9 ms. **b** Plotting head latency against head amplitude shows that these six sites (●) were associated with sites with minimal head movements, rendering detection of head onset problematic

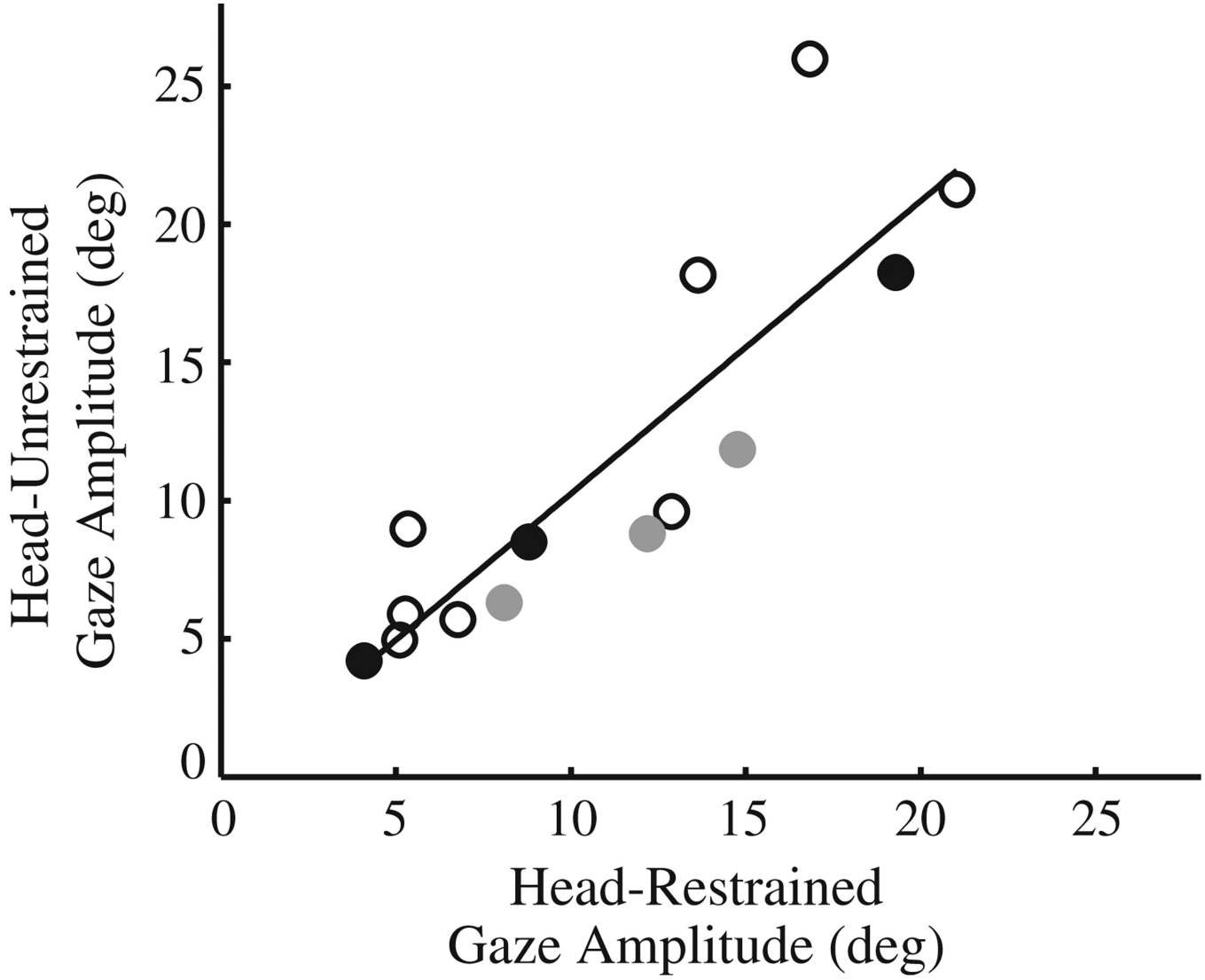

Fig. 5.

Comparison of stimulation-evoked changes in gaze in head-restrained and head-unrestrained conditions. The data are fitted with a linear regression (*solid line*; slope = 1.05; $r = 0.87$; $P < 0.0001$). Data are from 10 sites. The *open circles* indicate the 8 sites with only one configuration of stimulation parameters. For two sites (*black and gray circles*), data points for each of three sets of stimulation parameters are included. For the site shown in *filled gray circles*, the stimulation durations were 200, 300, and 400 ms (20 μA, 300 Hz). For the site represented with *filled black circles* (see Fig. 2), stimulation durations were 50, 100, and 200 ms (25 μA, 300 Hz)

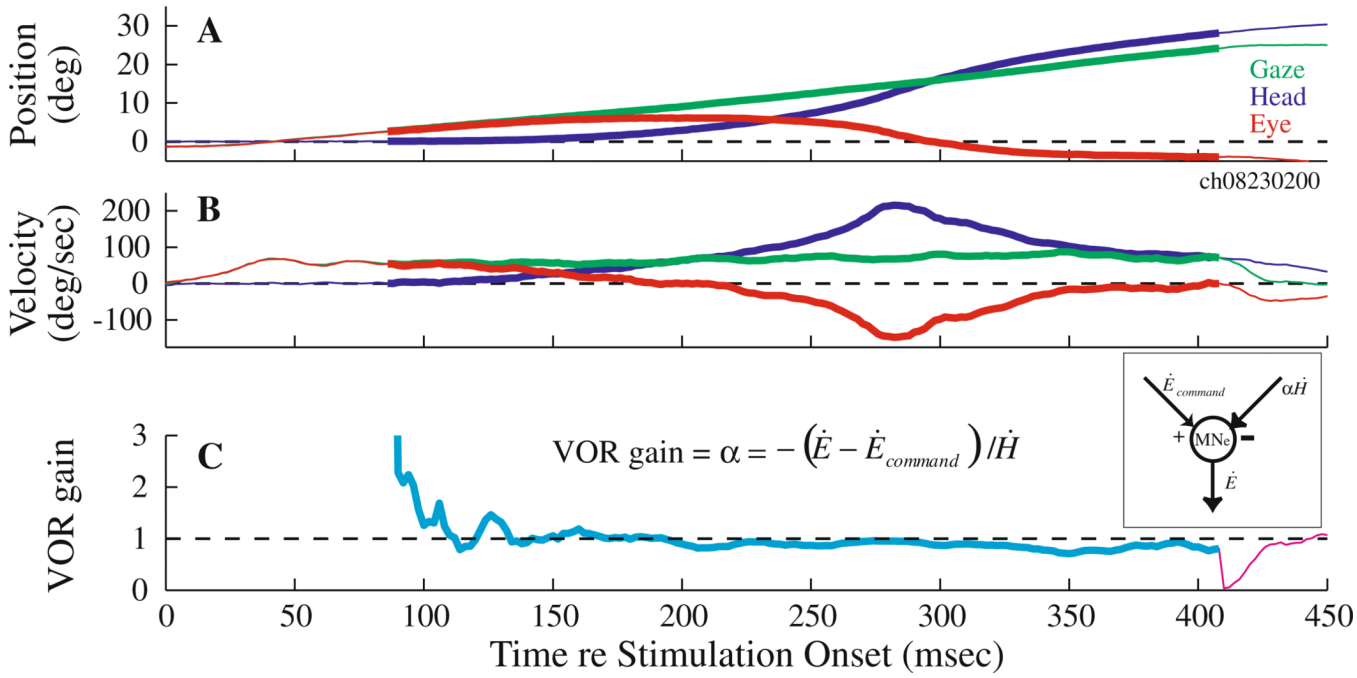

Fig. 6.

Example illustration of VOR gain computation during coordinated eye-head movements generated by PPRF stimulation. Temporal traces of the horizontal position (**a**) and velocity (**b**) of gaze (*green*), head (*blue*) and eye-in-head (*red*) components are shown for one trial. Plot starts at stimulation onset. The thick overlays on the traces mark the period from head movement onset to the end of the stimulation train. **c** The instantaneous VOR gain ($\alpha = -(\dot{E} - \dot{E}_{command})/\dot{H}$, see text for details) is plotted as a function of time. During the stimulation epoch (cyan trace), the velocity command ($\dot{E}_{command}$) equaled the constant velocity observed in the head-restrained condition at the same site and with identical stimulation parameters. It was set to zero after stimulation offset (*magenta trace*). The *inset* shows a schematic in which the output of the extraocular motoneurons incorporates an excitatory velocity input from the PPRF (saccade pathway) and an inhibitory velocity input due to the head movement (vestibular pathway)

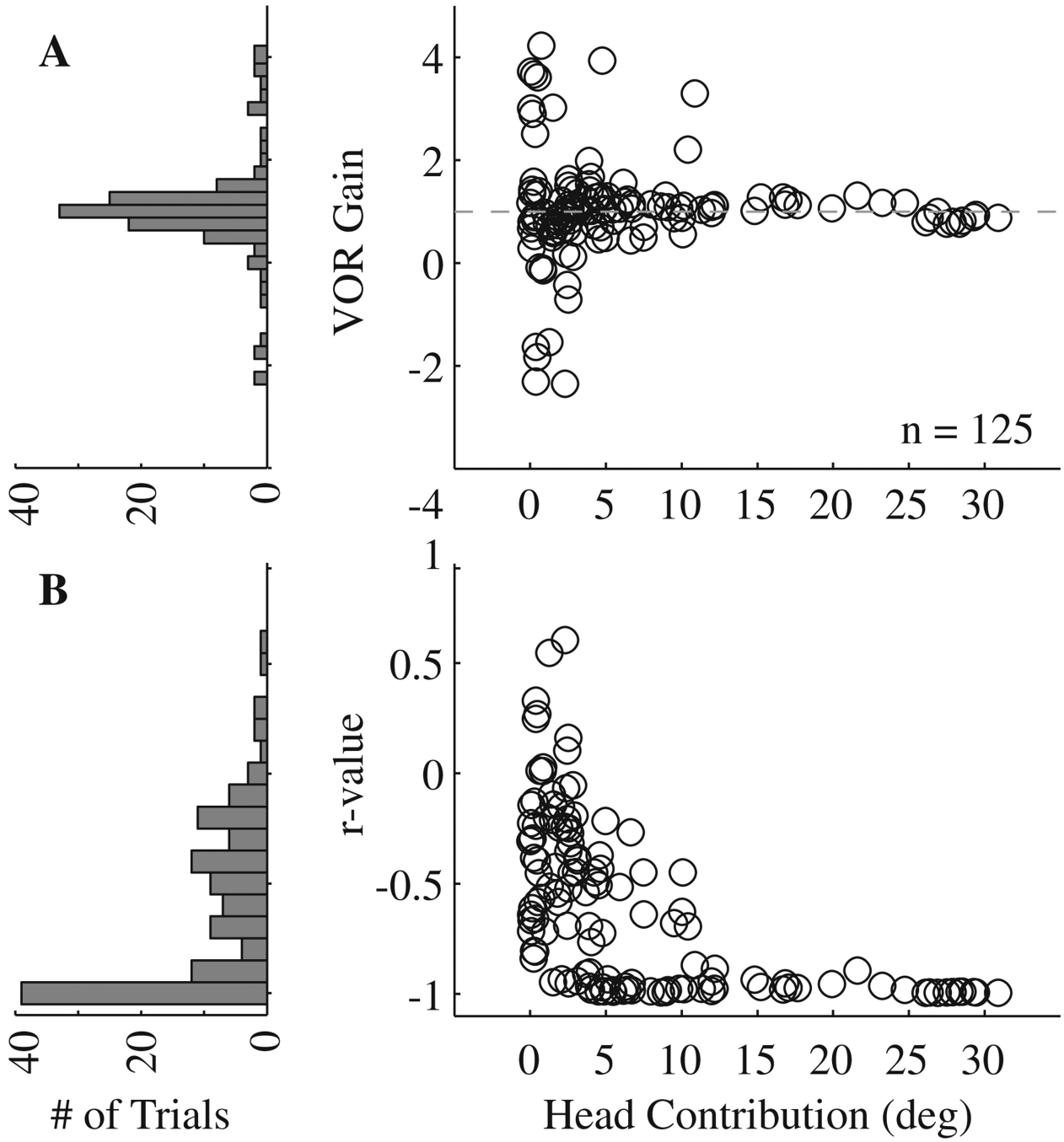

Fig. 7.

Results of the linear regression fits. **a** The estimated VOR gain is plotted in histogram format (*left*) and as a function of head contribution (*right*). The head contribution equals the displacement of the head during the change in gaze evoked by PPRF stimulation. The analysis was performed for the 125 trials across 10 stimulation sites. The *dashed horizontal line* indicates unity VOR gain. **b** The correlation coefficient or, the *r* value, of each individual linear fit is shown in the same format as **a**

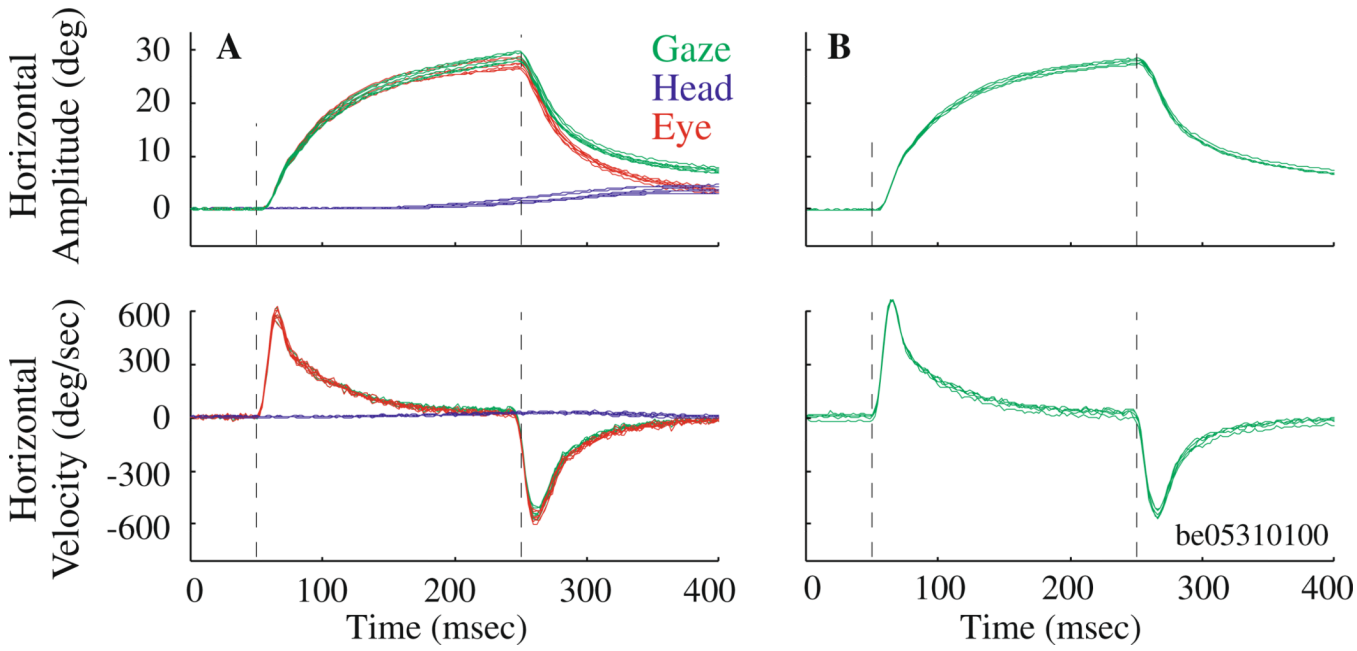

Fig. 8.

Microstimulation of the abducens nucleus in **a** head-unrestrained and **b** head-restrained conditions. **a** *Top* and *bottom panels* plot horizontal components of stimulation-evoked changes in position and velocity, respectively, in gaze (*green*), eye-in-head (*red*) and head-in-space (*blue*). **b** Same format at **a**, but only gaze profiles (*green*) are displayed; eye-in-head equals gaze because head-in-space is held constant at zero. Stimulation parameters: 25 μA, 200 ms, 300 Hz. *Vertical dashed lines* indicate stimulation onset and offset. These representative trials for both head-restrained (n = 5 trials) and head-unrestrained (n = 7 trials) data were evoked from the same site

Table 1

Linear regression parameters between ($\dot{E} - \dot{E}_{\text{command}}$) and $\dot{H}$

Site No.	No. of Trials	VOR gain Mean ± SD	Intercept Mean ± SD	Corr. coeff. Mean ± SD
be03030200	21	1.12 ± 0.16	8.21 ± 11.79	−0.98 ± 0.02 *
be03020400	9	0.81 ± 0.30	3.24 ± 5.56	−0.46 ± 0.13 *
be06090300	8	1.18 ± 0.08	−7.50 ± 3.05	−0.97 ± 0.01 *
be12070300	12	1.37 ± 0.86	−5.16 ± 16.46	−0.41 ± 0.15 *
be11280200	14	0.72 ± 1.34	−0.01 ± 31.34	−0.40 ± 0.48 *
be12140100	18	0.98 ± 1.46	−7.04 ± 5.10	−0.24 ± 0.34
be04280300	11	0.71 ± 0.15	−5.47 ± 3.04	−0.59 ± 0.07 *
be12080100	11	0.83 ± 2.17	−22.67 ± 6.96	−0.13 ± 0.29
ch08220200	11	1.08 ± 0.16	−2.05 ± 1.67	−0.90 ± 0.08 *
ch08230200	10	0.85 ± 0.08	2.09 ± 4.95	−0.99 ± 0.001 *

The VOR gain equals the negative of slope of the linear regression fit

* Statistically significant correlation (t-test, $P < 0.05$)